Vol. 35 (2004) *ACTA PHYSICA POLONICA B* No 6–7

RESULTS FROM SUPER-KAMIOKANDE AND K2K EXPERIMENTS*

Danuta Kiełczewska

for the Super-Kamiokande and K2K Collaborations

Institute for Experimental Physics, Warsaw University
and Sołtan Institute for Nuclear Studies
Hoża 69, 00-681 Warsaw, Poland
e-mail: danka@fuw.edu.pl

(Received May 5, 2004)

The Super-Kamiokande data from the first phase of the detector activity from April 1996 to July 2001 have been recently reanalysed and the new results are reported. Solar neutrino data allowed for precision analysis of oscillation parameters. When combined with the latest results from SNO and KamLAND experiments the best fit parameters of $\nu_e \leftrightarrow \nu_{\mu\tau}$ transitions are $\delta m^2 = (7.1^{+0.6}_{-0.5}) \times 10^{-5}$ eV^2 and $\tan^2\theta = 0.44 \pm 0.08$. The atmospheric neutrino sample is compared with the updated simulations taking into account flux calculations based on new primary cosmic ray measurements and modifications introduced to neutrino interaction model thanks to measurements in the near detectors of the K2K experiment. The new analysis based on a subsample of higher precision events allowed to reveal a dip in the distribution of the ratio of the distance over neutrino energy, presenting thus the first oscillatory behavior in neutrino data. As a result the parameters of the transitions $\nu_\mu \leftrightarrow \nu_\tau$ are better constrained: $1.9 \times 10^{-3} < \Delta m^2 < 3.0 \times 10^{-3}$ eV^2 and $\sin^2 2\theta > 0.90$ at 90% C.L. The atmospheric neutrino oscillations have been confirmed by the first long-baseline accelerator experiment, K2K, using the neutrino beam produced at KEK and interactions recorded in the Super-Kamiokande detector. The results from the phase I as well as phase II of the experiment show a deficit of muon neutrinos consistent with the atmospheric neutrino oscillations. Finally the most recent results on searches for proton decays are presented.

PACS numbers: 14.60.Pq, 14.60.Lm, 95.30.Cq, 95.55.Vj

---

* Presented at the Cracow Epiphany Conference on Astroparticle Physics, Cracow, Poland, January 8–11, 2004.

1. Introduction

During the last six years neutrino studies have revolutionized our ideas about leptons in the Standard Model of elementary particles. In 1998 the Super-Kamiokande (SK) Collaboration discovered oscillations [1] with the observation of a very pronounced angular anisotropy of the atmospheric muon neutrinos. The most natural origin of the oscillations are non-zero masses of neutrinos and mixing of various neutrino flavors. The mixing implies that flavor lepton numbers L_e, L_μ and L_τ are not conserved and requires an addition of right-handed neutrino states to the Standard Model of elementary particles. It is believed that small neutrino masses and neutrino mixing are generated by a new mechanism, beyond the Standard Model. The deficit of atmospheric neutrinos is best described by $\nu_\mu \leftrightarrow \nu_\tau$ oscillations.

A deficit of solar neutrinos have puzzled physicists since the first results of the Homestake chlorine experiment (see the review of early solar neutrino results in Ref. [2]). Missing electron neutrinos arriving from the Sun were later reported by other radiochemical experiments using gallium nuclei (for an updated list of references see Ref. [3]). The mistery of solar neutrinos was deepened by the SK experiment, which was the first to prove that the neutrino events point to the Sun direction and was able to measure energy and temporal distributions of the neutrino flux [4–6]. No modifications of the Standard Solar Model (SSM) [7] were able to explain the results and the oscillation hypothesis was widely accepted as the viable solution of the solar neutrino puzzle. However the final proof of the oscillation of electron neutrinos into a combination of muon and tau neutrino states, $\nu_e \leftrightarrow \nu_{\mu\tau}$, was provided by the SNO experiment. It was able to measure separately the ν_e flux via CC reactions [8] as well as the total flux of all flavors detecting neutrons from the NC deuterium disintegration. The neutrons were first detected via captures on deuterons [9] and most recently with the addition of salt to heavy water [10]. All solar observations are consistent with the scenario, in which ^{8}B electron neutrinos resonantly convert into a mass eigenstate by the large matter density inside the Sun. Consequently the ν_e leaving the Sun have the survival probability $\sim \sin^2\theta$ [11]. This almost pure eigenmass state arrives then to Earth, where it can be modified by Earth matter effects.

The oscillation parameters which provide the explanation for solar neutrino data can be probed by reactor antineutrinos at sufficiently large distances from a detector. The measurements by KamLAND found the evidence for $\overline{\nu_e}$ disappearance with the parameters consistent with the solar results [12]. The atmospheric neutrino results were confirmed by the K2K experiment, which has also observed the ν_μ disapearance using the accelerator neutrino beam at KEK [13].

The exciting search for solutions of the neutrino puzzles has thus been completed and with the firm evidence for neutrino oscillations we now start the first phase of precision measurements of the neutrino mass differences and mixing. In this report we will describe the current status of the studies of solar, atmospheric and accelerator neutrinos with the Super-Kamiokande (SK) detector.

The SK is a cylindrical 50 000 ton water Cherenkov detector. The water tank is optically separated into two concentric cylindrical detector regions. In its original configuration the inner detector (ID) was instrumented with 11146 inward facing 20 inch diameter photomultiplier tubes (PMT). The outer detector (OD) was instrumented with 1885 outward facing 8 inch PMTs. It is described in detail in Ref. [14].

SK measures the energy, direction and time of the charged products of neutrino interactions by detection of the emitted Cherenkov light. The data have been collected since April 1996. During the detector upgrade in the summer of 2001 an accident destroyed half of the photo-multipliers. The detector was rebuilt in 2002 and is now operating with about half of the original photocathode coverage. We therefore analyze separately the data before the accident, which are referred to as SK-I and the samples collected after December 2002, called SK-II. More details about the SK data analyses, in particular a reduction of 3-flavor mixing to 2-flavor oscillation formulae, can be found *e.g.* in Refs. [15, 16]. If not mentioned otherwise the analyses are based on a two flavor mixing assumption. This assumption is justified by the fact that $\Delta m^2_{\mathrm{atmos}} \gg \delta m^2_{\mathrm{solar}}$.

We will review the recent results of the updated analysis of the SK-I data for both solar (Sec. 2) and atmospheric neutrinos (Sec. 3). In the oscillation analysis of the SK solar data the new results of other experiments are used. The K2K data of the first (K2K-I) and second (K2K-II) phases of the experiment will be presented as well as first results of a search for electron appearance.

The SK detector is the most sensitive instrument for searches of proton decays. The updated limits on proton lifetime will be presented in Sec. 4.

2. Solar neutrinos

The solar ^{8}B neutrinos have energies below 14 MeV and therefore the only reaction available with light water is elastic scattering on electrons. The cross section is orders of magnitude smaller than for interactions on free (or quasi-free) nucleons but its characteristic forward scattered electrons allow for efficient extraction of a solar signal from background. With large SK statistics it is possible to separate solar signals in bins of energy and zenith angle of the Sun at the known time of the event occurrence. Study of the zenith angle dependence is important because of a possible regeneration of ν_e's caused by the passage through Earth matter due to the MSW effects. It is often described by the day/night rate asymmetry: $A_{\rm DN} = \frac{\rm D-N}{0.5(\rm D+N)}$, where D (N) refers to the neutrino interaction rate during the day (night).

The analysis is presented for data set consisting of 1496 live days (May 31, 1996 through July 15, 2001). The measured rate (normalized to SSM expectations) and day–night asymmetry dependence on the energy of recoil electrons is shown in Fig. 1.

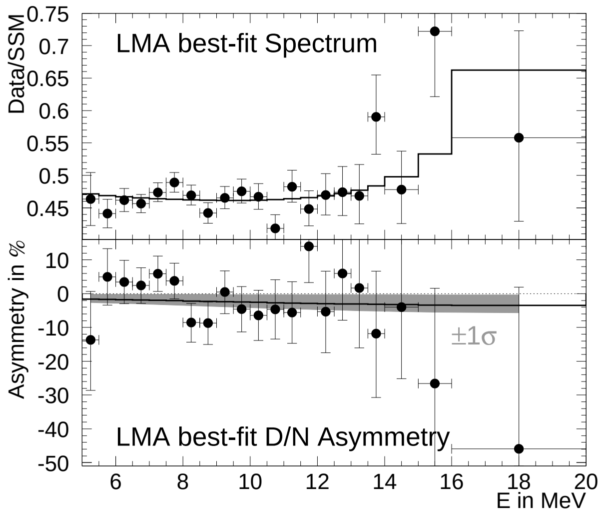

Fig. 1. The electron spectrum (top) and day-night asymmetry (bottom).The solid lines are expected distributions for $\delta m^2 = 6.3 \times 10^{-5}$ eV^2 and $\tan^2\theta = 0.55$. Each energy bin was fit independently to the rate (top) and the day–night asymmetry (bottom). The gray band is $\pm 1\sigma$ range corresponding to the fitted value over the entire energy range: $\rm A_{DN} = -1.8 \pm 1.6\%$.

No significant energy or zenith angle modulation has been observed. The apparent enhancement at large electron energies is an effect of the finite energy resolution. However the neutrino transformation during the night vary with oscillation parameters. Therefore, for the oscillation analysis a maximum likelihood fit was performed of the expected and observed rate variation with the solar zenith angle. The details of the analysis are described in Ref. [18, 19]. The SK data alone excludes small mixing at more than 3σ. It also disfavors $\delta m^2 > 10^{-3}$ eV^2 and 2×10^{-9}eV$^2 < \delta m^2 < 3 \times 10^{-5}$ eV^2.

Th SK zenith-angle and energy measurements can then be combined with the solar neutrino rates measured in all the other detectors, including the recent SNO salt-phase measurements [10]. The data were fitted without

SSM predictions. In Fig. 2 the area of acceptable parameters is overlaid with the allowed regions from the reactor KamLAND results. The latter come from a binned likelihood analysis [20]. Assuming the CPT invariance the neutrino and antineutrino oscillation parameters should be the same. One can see that solar data select one of a few regions of δm^2 acceptable by KamLAND. When all data are combined the best fit oscillation parameters are:

$$\delta m^2 = (7.1^{+0.6}_{-0.5}) \times 10^{-5}\ \mathrm{eV}^2 \quad \text{and} \quad \tan^2\theta = 0.44 \pm 0.08\,.$$

The day–night asymmetry averaged over the entire energy spectrum is $(-1.8 \pm 1.6(\mathrm{stat})^{+1.3}_{-1.2}(\mathrm{syst}))\%$.

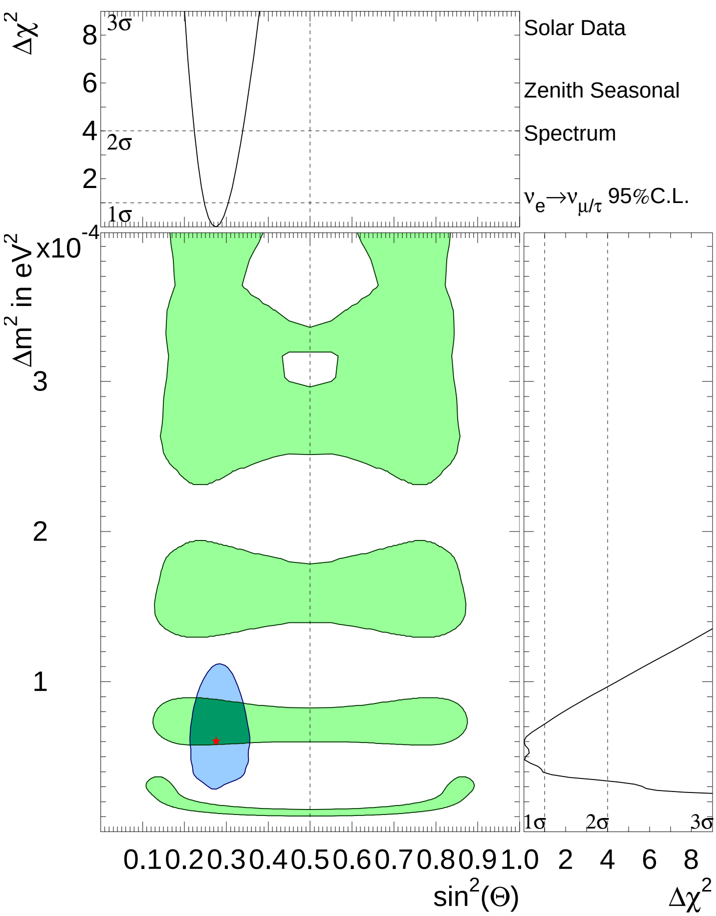

Fig. 2. Allowed regions at 95% c.l. from all solar and KamLAND data. The functions at the top and the right of each panel are the marginalized $\Delta\chi^2$ functions.

The SK-I data were also used to search for a signal of non-zero neutrino magnetic moment in a distortion of the energy spectrum of recoil electrons. An upper limit of $3.6 \times 10^{-10}\mu_B$ was set at 90% C.L. [21]. The data also allowed to search for electron antineutrinos coming from the Sun and an upper limit was set [22]. Finally no periodic modulation of the solar neutrino flux was found in SK-I data [23] contrary to findings by other authors.

3. Atmospheric neutrinos

The evidence for the atmospheric neutrino oscillations $\nu_\mu \leftrightarrow \nu_\tau$ has been derived so far from the observation of the muon neutrino disappearance. Its variation with the neutrino flight length L and energy E is very well described by the survival probability given by:

$$P(\nu_\mu \to \nu_\mu) = 1 - \sin^2 2\theta \sin^2 \left(\frac{1.27\Delta m^2(\mathrm{eV}^2)L(\mathrm{km})}{E(\mathrm{GeV})} \right) . \tag{1}$$

In the standard oscillation analysis this formula was fitted to the zenith angle distributions in several energy intervals.

However, the sinusoidal L/E dependence of the survival probability has not yet been observed. With the large SK samples an analysis was undertaken to select a sample of events with good resolution in L/E.

3.1. The L/E analysis

The SK-I data used here correspond to the exposure of 1489 live-days. Only the contained events were analyzed with the interaction vertex inside the fiducial volume (FV) of the detector. The direction and the momentum of charged particles were reconstructed from the Cherenkov ring image. Each observed ring was identified as either e-like or μ-like based on the shape of the ring pattern. Two classes of events were used: fully contained (FC) with all the visible energy deposited inside the ID and partially contained (PC) with some energy deposited also in the OD. In order to select a sample enhanced in muon neutrinos only the μ-like single-ring FC events were considered and those multi-ring FC events, when the most energetic particle was classified as μ-like. The same selection criteria were applied to a Monte Carlo (MC) sample of simulated events.

In order to increase the statistics the fiducial volume for the FC events was expanded from 22.5 ktons (in standard analysis) to 26.4 ktons. It is estimated that a non-neutrino background in the expanded fiducial volume is negligibly small, less than 0.1%. To get a better neutrino energy estimate from the PC events a special procedure was devised to select muons which stopped in the OD detector. Their energy was determined on the basis of the number of photoelectrons recorded in OD. For the remaining, "OD through-going" muons, the projected track length in the OD was used for the energy estimate. The neutrino energy was calculated for every event from a functional relationship between the neutrino and the observed energy found from MC simulation.

The flight length of neutrinos is derived from the zenith angle, Θ, of the reconstructed neutrino direction, taken to be along the total momentum vector from all observed particles. The worst neutrino energy reconstruction occurs for PC events of energies above 5 GeV (energy resolution more than 40%). However they are advantageous for flight path determination because of a very good correlation between neutrino and muon direction and a good reconstruction of muon direction. Interactions of low energy neutrinos have the worst angular resolution because of large transverse momenta of invisible recoil nucleons. The flight path is poorly reconstructed for all horizontal-going neutrinos due to large $dL/d\Theta$. Eventually the resolution cut of $\Delta(L/E) < 70\,\%$ was determined from the MC simulation to maximize the sensitivity to distinguish neutrino oscillation from other hypotheses (see Ref. [24] for details).

Numbers of events remaining after the 70% resolution cut are summarized in Table I.

TABLE I

Summary of atmospheric neutrino events used in the analysis. Only μ-like events are used. Numbers of the MC events are normalized by the live-time. Neutrino oscillation is not included in the MC. Numbers in the parentheses show the estimated fraction of $\nu_\mu + \overline{\nu}_\mu$ CC interactions in each sample.

		Data	MC	$\nu_\mu + \overline{\nu}_\mu$ CC
FC	single-ring μ-like	1619	2105.8	(98.3 %)
	multi-ring μ-like	502	813.0	(94.2 %)
PC	OD stopping	114	137.0	(95.4 %)
	OD through-going	491	670.4	(99.1 %)

Fig. 3 displays number of events as a function of L/E for the data and MC predictions. Below 150 km/GeV, the data and MC agree well, while the muon deficit is seen for higher values of L/E.

The ratio of the data points to the MC histogram from Fig. 3 is plotted in Fig. 4 as a function of L/E. The plot shows a dip around $L/E = 500$ km/GeV. Note that the position of the dip is about a factor of 3 to 4 away from that of the predicted event number minimum as seen in Fig. 3.

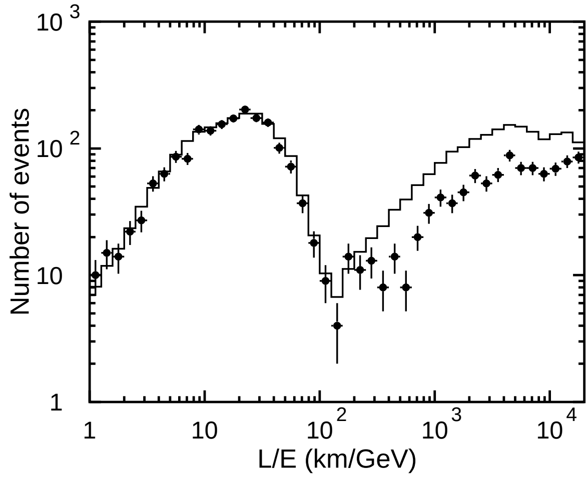

Fig. 3. Number of events as a function of reconstructed L/E for the data (points) and atmospheric neutrino MC events without oscillations (histogram). The MC histogram is normalized by the detector live-time.

The observed L/E distribution was fitted assuming $\nu_\mu \leftrightarrow \nu_\tau$ oscillations, taking into account 25 systematic uncertainties. The systematic terms are allowed to vary within the estimated errors which account for uncertainties in flux calculation, detector calibration, data reduction, event reconstruction, and neutrino interaction models. The best fit point was searched by scanning a $(\sin^2 2\theta, \log \Delta m^2)$ grid and minimizing χ^2 by optimizing the systematic error parameters at each point. The minimum χ^2 was 37.9/40 DOF at $(\sin^2 2\theta, \Delta m^2) = (1.00, 2.4 \times 10^{-3}\,\mathrm{eV}^2)$.

The best-fit expectation for 2-flavor $\nu_\mu \leftrightarrow \nu_\tau$ oscillations is shown by solid line in Fig. 4. The dip in the figure corresponds to the first maximum oscillation. Due to the poor L/E resolution, the second and higher oscillation maxima are not observed in this experiment.

In order to confirm that the observed dip was not due to systematic effects, different tests were carried out. Several L/E distributions were made by changing the L/E resolution cut value. Plots based on the resolution cuts at 60, 80 and 90% showed consistent dip structures as that based on the 70% cut. Also, L/E plots based on several other L/E bin sizes gave essentially the same results. In addition, the sign of the direction vector for each event was changed artificially. The L/E distribution for this artificial data sample did not show any significant dip structure. Finally, the L/E plot was made using FC single-ring e-like events. The e-like distribution was consistent with flat over the whole L/E range. Thus we are confident that the observed dip is not due to systematic effects in the event selection.

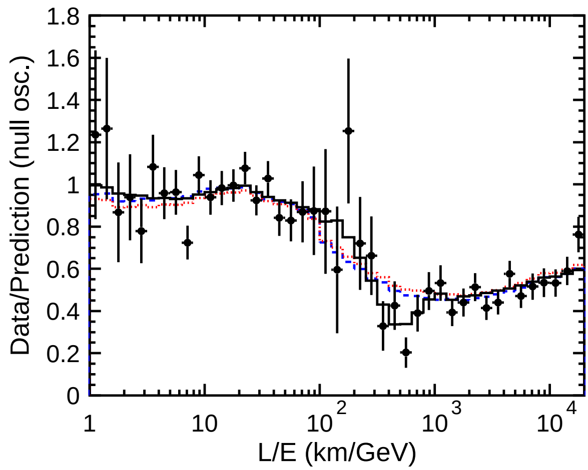

Fig. 4. Ratio of the number of events in data to the predicted by MC without neutrino oscillation (points) plotted as a function of the reconstructed L/E. Solid line histogram shows the best-fit expectation for 2-flavor $\nu_\mu \leftrightarrow \nu_\tau$ oscillations. The error bars are statistical only. Also shown are the best-fit expectations for neutrino decay (dashed line) and neutrino decoherence (dotted line).

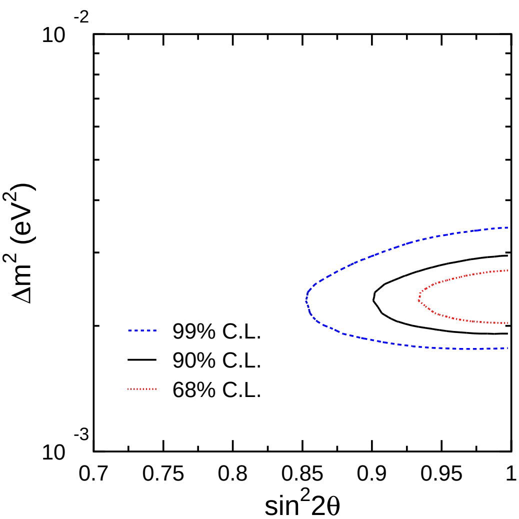

Fig. 5. Allowed oscillation parameter regions (68, 90 and 99% C.L.) for 2-flavor $\nu_\mu \leftrightarrow \nu_\tau$ oscillations.

Figure 5 shows the contour plot of the allowed oscillation parameter regions. Three contours correspond to the 68 %, 90 % and 99 % C.L. allowed regions, which are defined to be $\chi^2 = \chi^2_{\rm min} + 2.48$, 4.83, and 9.43, respectively, where $\chi^2_{\rm min}$ is the minimum χ^2 in the physical region. It is seen that at 90 % C.L. the parameters are constrained by: $1.9 \times 10^{-3}\,{\rm eV}^2 < \Delta m^2 < 3.0 \times 10^{-3}\,{\rm eV}^2$ and $\sin^2 2\theta\ > 0.90$.

In order to test the significance of the dip in L/E, a null hypothesis that includes the basic shape of the L/E distribution is needed. The no-oscillation case was very strongly disfavored by the data at large L/E. We used two alternative hypotheses that basically reproduce the zenith angle dependent deficit, predicting that about half of muon neutrinos smoothly disappear at large L/E. These hypotheses are neutrino decay [25, 26] and neutrino decoherence [27]. The former allows for the eigenmass state not participating in solar oscillations to decay to a sterile state, while the latter assumes that quantum gravitation effects destroy coherence of two oscillating states. Figure 4 includes the L/E distribution for the best-fit expectation for neutrino decay and neutrino decoherence. The obtained $\chi^2_{\rm min}$ values were 11.3 (3.4 standard deviations) and 14.5 (3.8 standard deviations) larger than $\chi^2_{\rm min}$ for neutrino oscillation.

3.2. Test of CPT violation

Atmospheric neutrinos and antineutrinos are produced with comparable rates. The large sample of atmospheric neutrino data made possible a CPT violation test by looking for a difference between the masses of neutrinos and antineutrinos. The data were fitted with $\Delta m^2(\nu)$ and $\Delta m^2(\overline{\nu})$ as independent parameters. The difference $\delta \equiv \Delta m^2(\nu) - \Delta m^2(\overline{\nu})$ is then constrained at 99% C.L.: $-0.0075\ {\rm eV}^2 < \delta < 0.0055\ {\rm eV}^2$ assuming maximal mixing. The constraint is slightly less restrictive than obtained in Ref. [28] from comparison of solar and reactor data: $|\Delta m^2(\nu) - \Delta m^2(\overline{\nu})| < 0.0013\ {\rm eV}^2$ but much stricter than the limit obtained for hadrons:$|m^2(K^0) - m^2(\overline{K^0})| < 0.25\ {\rm eV}^2$.

4. K2K long-baseline experiment

After the discovery of the atmospheric neutrino oscillations an independent check using a controlled accelerator beam became essential. An obvious option was to take advantage of the world's largest neutrino detector, SK, and the KEK accelerator at a distance of 250 km. This led to the K2K (KEK to Kamioka) experiment [29], which started to collect data in June 1999. In order to probe the region of $\Delta m^2 \sim 3 \times 10^{-3}\ {\rm eV}^2$ the neutrinos of energy about 1 GeV were needed. With such a small energy only the ν_μ disappearance can be studied, since a production of tau lepton is not possible. For best determination of original neutrino beam parameters a set of near detectors at KEK laboratory was constructed. To reduce uncertainties coming from neutrino interaction models two of the detectors use water as targets; one of them is 1 kton water Cherenkov (1KT) and another uses scintillating fibers around water containers.

The K2K neutrino beam originates from 12 GeV energy protons from the KEK Proton Synchrotron. Every 2.2 s about 6×10^{12} protons form a 1.2 μs beam pulse composed of 9 bunches. Positive pions are focused by pair of horn magnets operated at 250 kA. Neutrino beam mainly comes from $\pi^+ \rightarrow \nu_\mu \mu^+$ decays inside 200 m long decay tunnel, while muons are stopped in a dump. As a result 98% of the beam neutrinos are ν_μ with an estimated 1.3% of ν_e beam contamination. More details can be found in Ref. [30].

In the first phase of the experiment, K2K-I, the data was taken from June 1999 to July 2001, while K2K-II sample contains data from January 2003 to April 2003. The events associated with the K2K beam are extracted from SK data taking advantage of the timing information about each beam spill using Global Positioning System. The detection time at SK site corrected by the neutrino time of flight has to match the beam spill extraction time and its width of 1.2 μs.

Number of events predicted to be observed in absence of neutrino oscillation is calculated based on measurement in the near detectors. Table II contains comparison of predicted and observed number of events at SK. It describes K2K-I and K2K-II experiments phases corresponding to 4.8×10^{19} and 1.5×10^{19} accumulated protons on target respectively.

TABLE II

Summary of K2K results. The expected number of events is for no oscillation case and "p.o.t" stands for protons on target, which is used as a measure of the integrated beam intensity.

	K2K-I Jun'99–Jul'01	K2K-II Jan'03–Apr'03
p.o.t	4.8×10^{19}	1.5×10^{19}
Observed at SK	56	16
Expected from 1KT	$80.1^{+6.2}_{-5.4}$	$26.4^{+2.3}_{-2.1}$
Obs/Exp	0.70 ± 0.09(stat)	0.61 ± 0.15(stat)

The number of events expected in SK in case of no neutrino oscillations is calculated on the basis of 1KT measurements obtained with the same detector technique and reconstruction algorithms. In order to take into account a small change in the neutrino spectrum at the SK site as well as the fact that the neutrinos do not originate at one point, the beam simulation was used and tested by the beam monitors. The simulation of the neutrino interactions was tuned to the data from near detectors.

The oscillation analysis was performed for the K2K-I sample fitting both the observed event rate and shape of energy spectrum with the maximum-likelihood method. A detailed description of the analysis can be found in Ref. [13, 31].

Fig. 6 shows contours of the allowed oscillation parameter regions. They are consitent with SK-I atmospheric neutrino results [32]. For maximum mixing one gets $1.5\times10^{-3} < \Delta m^2 < 3.9\times10^{-3}$ at 90% C.L. The probability of no oscillations scenario is less than 1%.

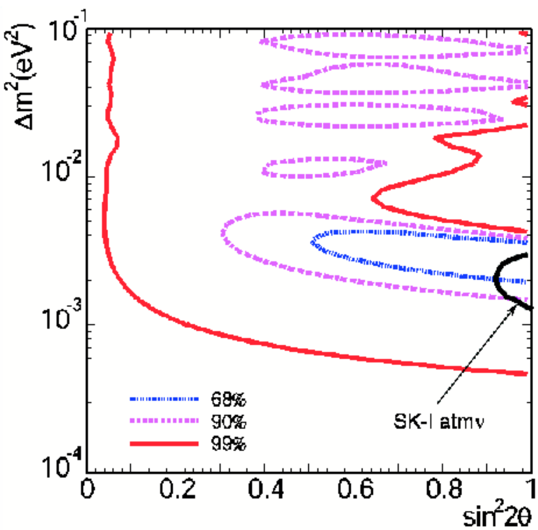

Fig. 6. Contours of the allowed oscillation parameter regions (68, 90 and 99% C.L.) explaining the K2K ν_μ disappearance. The SK-I atmospheric neutrino results (conventional analysis) are overlaid for comparison.

On top of the μ-like events discussed above one e-like event was observed in the K2K-I sample. The expected background in the absence of neutrino oscillations is estimated to be 2.4 ± 0.6 events and is dominated by mis-identification of events from neutral current π^0 production. This allows to exclude $\nu_\mu \leftrightarrow \nu_e$ appearance with parameters: $\sin^2 2\theta_{\mu e} > 0.15$ for $\Delta m^2 = 2.8\times10^{-3}\mathrm{eV}^2$ at 90% C.L. [1] The most stringent limit of $\sin^2 2\theta_{\mu e} < 0.09$ is obtained at $\Delta m^2 = 6\times10^{-3}$ eV^2 [33].

The K2K-I statistics should be doubled up to the total of 10^{20} protons on target before the scheduled end of the experiment in April 2005, which will result in a more statistically significant study of the shape of the energy spectrum.

[1] Note that $\sin^2 2\theta_{\mu e} = 2\sin^2\theta_{13}$ for $\sin^2 2\theta_{23} = 1$ using the conventional notation [16].

The SK detector will be subsequently used in the T2K (Tokai to Kamioka) off-axis experiment with the neutrino beam produced by 50 GeV protons from a very powerful accelerator JPARC (0.77 MW). Its main purpose is to study θ_{13} mixing angle with 20 times improved sensitivity than K2K [34]. Its commissioning is planned for 2009.

5. Search for proton decays

We found no evidence for nucleon decay mode in the SK-I sample. The preliminary lower limits of partial nucleon lifetime at 90% C.L. are shown in Fig. 7. They are obtained from analyses of various data fractions indi-

Summary of Nucleon Decay Searches

mode	exposure (kt• yr)	εB_m (%)	observed event	B.G.	τ/B limit (10^{32} yrs)
$p \to e^+ + \pi^0$	92	43	0	0.2	57
$p \to \mu^+ + \pi^0$	92	32	0	0.4	43
$p \to e^+ + \eta$	45	17	0	0.3	11
$p \to \mu^+ + \eta$	45	12	0	0	7.8
$n \to \bar{\nu} + \eta$	45	21	5	9	5.6
$p \to e^+ + \rho$	61	6.8	0	0.6	6.1
$p \to e^+ + \omega$	61	3.3	0	0.3	2.9
$p \to e^+ + \gamma$	70	71	0	0.1	73
$p \to \mu^+ + \gamma$	70	60	0	0.2	61
$p \to \bar{\nu} + K^+$	92				20
$K^+ \to \nu\mu^+$ (spectrum)		33	--	--	5.5
prompt $\gamma + \mu^+$		8.7	0	0.3	12
$K^+ \to \pi^+\pi^0$		6.5	0	0.9	8.6
$n \to \bar{\nu} + K^0$	79				3.0
$K^0 \to \pi^0\pi^0$		9.6	25	33.8	3.2
$K^0 \to \pi^+\pi^-$		4.6	10	6.7	1.1
$p \to e^+ + K^0$	70				5.4
$K^0 \to \pi^0\pi^0$		11.8	1	1.4	8.8
$K^0 \to \pi^+\pi^-$					
2-ring		6.2	6	1.0	1.5
3-ring		1.4	0	0.2	1.4
$p \to \mu^+ + K^0$	70				10
$K^0 \to \pi^0\pi^0$		6.1	0	1.1	6.2
$K^0 \to \pi^+\pi^-$					
2-ring		5.3	0	1.5	5.4
3-ring		2.8	1	0.2	1.8

Fig. 7. Limits on partial lifetime limits for various decay modes. B_m stands for the mode branching ratio, ϵ is the efficiency (in %), and B.G. is background from atmospheric neutrinos.

cated by the exposure values. A paper with the results for decays via modes involving kaons, which are favored by supersymmetric grand unified models is currently under preparation for the whole SK-I sample of 1489 days corresponding to the exposure of 99 kt-years.

The procedures used for candidate selection and background estimates can be found in Refs. [35, 36].

6. Conclusions

With the SNO experiment sensitivity to different processes and large statistics of SK data the solar neutrino puzzle is now solved by the $\nu_e \leftrightarrow \nu_{\mu\tau}$ oscillations. When KamLAND $\overline{\nu_e}$ reactor data are added the amazing precision of the oscillation parameters is achieved (assuming CPT invariance): $\delta m^2 = (7.1^{+0.6}_{-0.5}) \times 10^{-5}$ eV^2 and mixing at $\tan^2\theta = 0.44 \pm 0.08$. The mixing angle is thus significantly different from maximal.

Using a subsample of SK-I atmospheric neutrino data with higher precision in the L/E variable we found an evidence for an oscillatory signature. The survival probability of muon neutrinos shows a dip corresponding to the first oscillation maximum.

This analysis strongly constrains Δm^2. The best fit values of the oscillation parameters are $(\sin^2 2\theta,\, \Delta m^2) = (1.00,\, 2.4 \times 10^{-3}\,\mathrm{eV}^2)$. At 90 % C.L. the parameters are constrained by: $1.9 \times 10^{-3}\,\mathrm{eV}^2 < \Delta m^2 < 3.0 \times 10^{-3}\,\mathrm{eV}^2$ and $\sin^2 2\theta \; > 0.90$. This implies that at least one of the neutrino masses is larger than 44 meV.

The K2K experiment confirms the findings of atmospheric neutrino studies. It also provides unique experience for the future long-baseline experiment, T2K, which is going again to take advantage of the SK detector. It's planned that it will be able to probe the mixing matrix element $|U_{e3}|^2$ down to 0.0015 for the current best fit value of Δm^2.

With the perspective of the future project the SK detector will be rebuilt and brought back to its original photocathode coverage with about 12000 PMTs in 2006.

The SK-I sample with the achieved exposure of 99 kton-years provide unique data to search for proton decays. With no evidence for proton decay the lower lifetime limits are set. For many expected decay modes the limits are of the order of 10^{33} years and serve as the main source of tests for grand unified models.

The Super-Kamiokande and K2K Collaborations acknowledge the cooperation of the Kamioka Mining and Smelting Company. Both experiments have been built and operated from funding by the Japanese Ministry of Education, Culture, Sports, Science and Technology, the United States Department of Energy, and the U.S. National Science Foundation. The author gratefully acknowledges the support of the Polish State Committee for Scientific Research, grant number 1P03B03826. The author is thankful to organizers for the kind invitation and the hospitality extended to her at the workshop.

REFERENCES

[1] Y. Fukuda *et al.*, *Phys. Rev. Lett.* **81**, 1562 (1998).

[2] J.N. Bahcall, *Neutrino Astrophysics*, Cambridge University Press, 1989.

[3] S.M. Bilenky, `hep-ph/0402153`.

[4] Y. Fukuda *et al.*, *Phys. Rev. Lett.* **81**, 1158 (1998); Erratum, *Phys. Rev. Lett.* **81**, 4279 (1998).

[5] Y. Fukuda *et al.*, *Phys. Rev. Lett.* **82** 2430, (1999).

[6] Y. Fukuda *et al.*, *Phys. Rev. Lett.* **82**, 1810 (1999). Y. Fukuda *et al.*, *Phys. Rev. Lett.* **85**, 3999 (2000).

[7] J.N. Bahcall, M.H. Pinsonneault, S. Basu, *Astrophys. J.* **555**, 990 (2001); A.S. Brun, S. Turck-Chieze, P. Morel, *Astroph. J.* **506**, 913 (1998).

[8] Q.R. Ahmad *et al.*, *Phys. Rev. Lett.* **87**, 071301 (2001).

[9] Q.R. Ahmad *et al.*, *Phys. Rev. Lett.* **89**, 011301 (2002).

[10] Q.R. Ahmad *et al.*, `nucl-ex/0309004`, to be published in *Phys. Rev. Lett.*

[11] S.P. Mikheev. A.Y. Smirnov, *Sov. J. Nucl. Phys.* **42**, 913 (1985); *Nuovo Cim.* **9C**, 17 (1986); L. Wolfenstein, *Phys. Rev.* **D17**, 2369 (1978).

[12] K. Eguchi *et al.*, *Phys. Rev. Lett.* **90**, 021802 (2003).

[13] S.H. Ahn *et al.*, *Phys. Rev. Lett.* **90**, 041801 (2003).

[14] S. Fukuda *et al.*, *Nucl. Instrum. Methods Phys. Res.* **A501**, 418 (2003).

[15] D. Kiełczewska [Super-Kamiokande and K2K Collaborations], *Acta Phys. Pol. B* **31**, 1181 (2000).

[16] D. Kiełczewska [Super-Kamiokande and K2K Collaborations], *Acta Phys. Pol. B* **33**, 189 (2002).

[17] A. Junghans *et al.*, *Phys. Rev.* **C68**, 065803 (2003); J. Bahcall *et al.*, *Astrophys. J.* **555**, 990 (2001).

[18] M. Smy *et al.*, *Phys. Rev.* **D69**, 011104 (2004).

[19] M. Smy, `hep-ex/0310064`.

[20] A. Ianni, *J. Phys. G: Nucl. Part. Phys.* **29**, 2107 (2003).

[21] D.W. Liu *et al.*, `hep-ex/0402015`, submitted to *Phys. Rev.*

[22] Y. Gando *et al.*, *Phys. Rev. Lett.* **90**, 171302 (2003).

[23] J. Yoo *et al.*, *Phys. Rev.* **D68**, 092002 (2003).

[24] Y. Ashie *et al.*, `hep-ex/0404034`, submitted to *Phys. Rev. Lett.*

[25] V.D. Barger, J.G. Learned, S. Pakvasa, T.J. Weiler, *Phys. Rev. Lett.* **82**, 2640 (1999).

[26] V.D. Barger, *Phys. Lett.* **B462**, 109 (1999).

[27] G.L. Fogli, E. Lisi, A. Marrone, *Phys. Rev.* **D67**, 093006 (2003).

[28] H. Murayama, `hep-ph/0307127`.

[29] S.H. Ahn *et al.* , *Phys. Lett.* **B511**, 178 (2001).

[30] J. Zalipska, *Acta Phys. Pol. B* **35**, 1231 (2004).

[31] I. Kato for K2K Collaboration, talk at Electroweak Interactions and Unified Theories, Moriond, France, 15-22 March, 2003; `hep-ex/0306043`.

[32] Y. Suzuki for the SK Collaboration, talk at The 28$^{\text{th}}$ International Cosmic Ray Conference, Tsukuba, Japan, July 31–August 7, 2003.

[33] M.H. Ahn *et al.*, `hep-ex/0402017`, submitted to *Phys. Rev. Lett.*

[34] Y. Itow *et al.*, LOI for JHF-ν experiment (2001), `hep-ex/0106019`.

[35] M. Shiozawa *et al.*, *Phys. Rev. Lett.* **81**, 3319 (1998).

[36] S. Mine for the Super-Kamiokande Collaboration, *Nucl. Phys. Proc. Suppl.* **112**, 154 (2002).